ELSEVIER

Journal of Electron Spectroscopy and Related Phenomena 106 (2000) 141–151

JOURNAL OF ELECTRON SPECTROSCOPY and Related Phenomena

www.elsevier.nl/locate/elspec

Cluster size effects upon anion solvation of N-heterocyclic molecules and nucleic acid bases

V. Periquet, A. Moreau, S. Carles, J.P. Schermann, C. Desfrançois*

Laboratoire de Physique des Lasers, U.M.R. 7538, C.N.R.S., Institut Galilée, Université Paris Nord, F-93430 Villetaneuse, France

Abstract

Rydberg electron transfer spectroscopy is used for the experimental determination of slightly negative electron affinities of N-heterocyclic molecules, pyridine, pyridazine, pyrimidine, pyrazine and DNA bases, adenine, cytosine, thymine and uracil. These molecules are solvated inside clusters of rare gases, water, ammonia or toluene in order to stabilize their anions against autodetachment, and the anion formation process is studied as a function of the number of solvent atoms or molecules. Determination of the cluster size thresholds above which valence anions are observed provides estimations of the electron affinities which are compared with the results of other experimental or theoretical determinations.

Keywords: DNA bases; electron affinities; solvation; cluster anions

1. Introduction

Electron affinities play a key role in electron transfer processes occurring in the gas-phase (discharges, atmospheric chemistry . . .) or in the condensed phase (electrochemistry, biochemistry . . .). While measurements and quantum calculations [1] of atomic electron affinities have now reached a high degree of accuracy, the situation is much less favorable for molecular species [2,3]. In some cases, not only the magnitude but even the sign of some valence molecular electron affinities are difficult to establish. Due to intranuclear rearrangement upon ionization, the molecular case is indeed much more complex and exhibits many different anion states in the gas-phase. A free electron, temporarily captured by a neutral molecule M (vertical Franck–Condon transition), gives birth to a negative ion $M^{-(*)}$ which is often rather highly vibrationally excited (see Fig. 1). The equilibrium geometry of M^- is indeed generally different from that of M because the capture of the excess electron in an unfilled valence orbital causes nuclear geometry modifications. In absence of any surrounding, temporary valence anions can survive to autodetachment during lifetimes ranging from fractions of a picosecond up to more than milliseconds. The internal energy can be removed by an eventual environment, e.g. in solution or inside a van der Waals cluster, leading to a more or less relaxed anion. More quantitatively, at least three energetic quantities, the vertical and adiabatic electron affinities (EA_v and EA_{ad}) and the vertical detachment energy (VDE), can be measured, as defined on Fig. 1. If the adiabatic electron affinity is positive, i.e. if the ground state of the anion lies below that of the neutral, definitely stable negative ions can be formed experimentally. In that case, photoelectron spectroscopy experiments generally

*Corresponding author.

0368-2048/00/$ – see front matter
PII: S0368-2048(99)00072-9

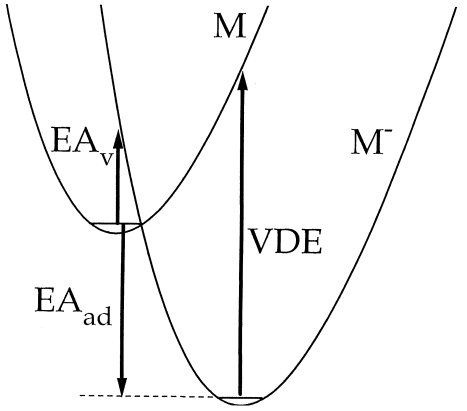

Fig. 1. Definition of the energetic quantities for molecular anions. In this figure, the horizontal axis corresponds to an intramolecular coordinate. The adiabatic EA_{ad} or vertical EA_v electron affinities are the differences between the ground state energy of the molecule and the ground state energy of the molecular anion or its potential energy at the equilibrium geometry of the neutral. They are generally counted positively downstairs, i.e. $EA_v<0$ and $EA_{ad}>0$ in this figure. The vertical detachment energy is defined as the difference between the potential energy of the neutral molecule at the equilibrium geometry of the anion and the ground state anion energy. It is always positive for stable anions.

allow for the precise determination of both VDE and EA_{ad} values [4,5].

On the other hand, mainly two different experimental techniques have been employed for the determination of negative molecular electron affinities. Electron attachment energies in the gas-phase can be determined by means of electron transmission spectroscopy (ETS) through the observation of resonances corresponding to temporary negative ion formation [6–10]. The assignment of the anion vibrational states is difficult when the transmitted electron energies become very small, i.e. when the electron affinity is close to zero, or when the autodetachment lifetimes are so small that only very broad resonances are observed. Measured resonant electron energies can thus be interpreted as the negative of either vertical or adiabatic electron affinities. The reversible reduction potentials of many molecules in solution have been measured in cyclic voltametry experiments [11] and a correlation has been suggested between those measured values and the corresponding adiabatic electron affinities EA_{ad}. The main assumption of this method is that the solvation energies are constant or at least depend linearly on the electron affinities, within a family of 'similar' molecules. As is discussed below, this is however questionable and some of the obtained values are in contradiction with recent ETS results [10] and the present work.

Quantum chemists also experience difficulties in the determination of negative electron affinities [2]. Variational calculations do not apply to unstable anion states which are a matter for quantum scattering theories. Those are unfortunately computationally very demanding and have been restricted only to small species, such as N_2^- or CO_2^-. With the use of the Koopmans' theorem associated with a proper scaling to some known experimental values [12], one can hope to reach a level of prediction at a level of precision similar to experimental uncertainties, i.e. 0.1 eV or less. This is probably true for the vertical electron affinities of the π^* anion states of simple hydrocarbons [13] but this becomes more questionable for vertical or adiabatic electron affinities of more complex molecules like DNA bases [10,14]. In that case, the presence of different electrophilic substituents and different π orbitals makes such predictions more uncertain, with typical discrepancies of the order of 0.2 eV or more.

The aim of this work was to experimentally determine gas-phase negative electron affinities of two sets of molecules which have been experimentally investigated by means of ETS [6–10] and used for scaling of experimental data [12,14]. The first set contains N-heterocyclic (azine) molecules (pyridine, pyridazine, pyrimidine and pyrazine), in which the formation of anion states is the result of the electron capture into the delocalized π^* orbital and is influenced by substitutions in the benzene ring. The second set corresponds to four of the five nucleic acid bases: uracil, thymine, cytosine and adenine. We were unsuccessful with guanine due to the difficulty of getting a high enough vapor pressure of this molecule without isomerization or decomposition. Our experimental approach is intermediate between gas-phase (ETS) and solution experiments: we choose to determine electron attachment properties of these molecules embedded inside clusters of different solvent species, as a function of the cluster size. By stepwise cluster solvation, initially unstable anions are stabilized and become observable as stable valence anions above a critical number of

solvent species. The interpretation of these experimental thresholds for stable cluster anions, with the help of calculated solvation energies, will allow us to infer the electron affinities of the isolated molecules. We first describe this method in some detail, the semi-empirical calculations which are performed to determine the cluster solvation energies and the experimental procedure which allows us to produce and to characterize cluster anions. We then present and analyze the obtained experimental data and we discuss the deduced electron affinities. The molecules studied here possess large dipole and/or quadrupole moments and some of them or their clusters can thus possibly give birth to dipole-bound anions, i.e. anions into which excess electrons are captured in a very diffuse orbital nearly totally localized outside the molecular frame [2]. In this work, we will not consider this electron binding process and will restrict the discussion to conventional valence anions.

2. Cluster solvation method

2.1. Principle

Our aim is the determination of the valence electron affinity EA of an isolated molecule M. If it is positive, we observe a stable negative ion M^- of the bare molecule and our experimental approach does not provide us any mean of quantitative determination. If it is negative, cluster solvation will stabilize M^- with respect to M so that the electron affinity of the cluster $M(S)_N$ can eventually become positive above a threshold number N_{th} of solvent species S [15]. We will thus observe stable solvated anions $M^-(S)_N$ for all N-values larger than N_{th}. The electron affinity EA of the isolated molecule is related to the electron affinity EA(N) of the mixed $M(S)_N$ cluster by the following relationship (see Fig. 2):

$$\mathrm{EA}(N) = \mathrm{EA} + E_{\mathrm{sol}}^{\mathrm{M}^-}(N) - E_{\mathrm{sol}}^{\mathrm{M}}(N) \qquad (1)$$

where $E_{\mathrm{sol}}^{\mathrm{M}^-}(N)$ and $E_{\mathrm{sol}}^{\mathrm{M}}(N)$ are the (positive) solvation energies of M^- and M surrounded by N solvent species. Due to the interactions brought by the presence of the extra electron, $E_{\mathrm{sol}}^{\mathrm{M}^-}(N)$ is always larger than $E_{\mathrm{sol}}^{\mathrm{M}}(N)$ and the difference increases with N, at least for sufficiently low N-values for which a total screening of the anion charge is not achieved. The electron affinity of the mixed cluster becomes positive when the number of solvents is equal or larger than a threshold value N_{th}

$$\mathrm{EA}(N_{\mathrm{th}}) \geq 0 \text{ and } \mathrm{EA}(N_{\mathrm{th}} - 1) \leq 2 \qquad (2)$$

Those two relations lead to a bracketing of EA when using the above Eq. (1):

$$E_{\mathrm{sol}}^{\mathrm{M}}(N_{\mathrm{th}}) - E_{\mathrm{sol}}^{\mathrm{M}^-}(N_{\mathrm{th}}) \leq \mathrm{EA} \leq E_{\mathrm{sol}}^{\mathrm{M}}(N_{\mathrm{th}} - 1) - E_{\mathrm{sol}}^{\mathrm{M}^-}(N_{\mathrm{th}} - 1) \qquad (3)$$

where EA is a negative value.

In the above expressions we do not specify whether electron affinities and solvation energies are adiabatic ones, i.e. energy differences between fully relaxed bare or solvated neutrals and anions, or vertical ones, i.e. the energy differences between neutrals and anions at the equilibrium geometry of the neutrals. We also implicitly assume that the excess electron is totally localized on the molecule M, i.e. that the solvent species are totally inert with respect to electron attachment. These important points will be discussed in Section 3.2.

2.2. Calculation of solvation energies

This method requires the evaluation of the solvation energies of the neutral and the negatively charged species. In order to investigate the structure and the energetic of the considered mixed clusters, we use a semi-empirical model for the intermolecular potential energies. It will be described and discussed in more detail elsewhere [16] but we here present its main characteristics. It is built with pairwise additive interatomic interactions, plus a many-body polarization term for each atom. The sum of electrostatic and Lennard–Jones 6–12 terms is used for the construction of interatomic potentials V_{ij}

$$V_{ij} = \frac{e^2}{4\pi\varepsilon_0}\frac{q_i q_j}{r_{ij}} + 4\varepsilon_{ij}\left[\left(\frac{\sigma_{ij}}{r_{ij}}\right)^{12} - \left(\frac{\sigma_{ij}}{r_{ij}}\right)^{6}\right] \qquad (4)$$

where r_{ij} is the interatomic distance, q_i and q_j are the

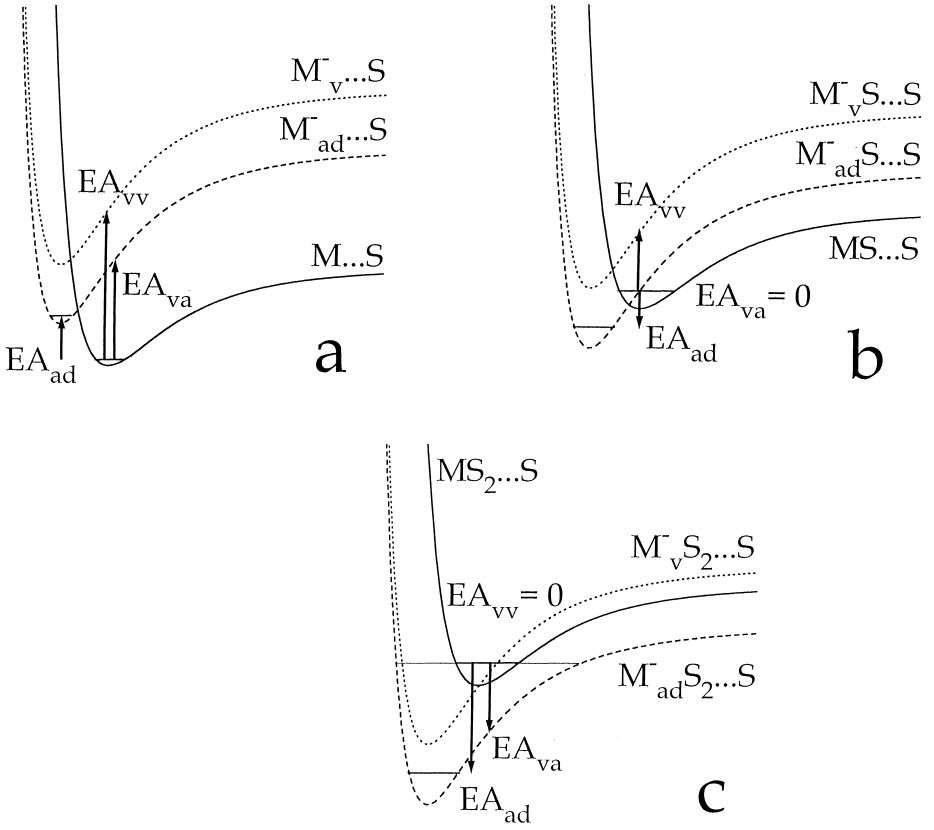

Fig. 2. Schematic of the stepwise solvation of a molecular species M and *N*V, where M initially possesses a negative electron affinity, represented as a function of the successive intermolecular coordinates between M, MS, MS_2 and a solvent species S. The horizontal axis corresponds to an intermolecular coordinate M . . . S. The intramolecular coordinates of M are taken into account only through the two adiabatic M^-_{ad} and vertical M^-_v energy levels of the molecular anion. The vertical axis corresponds to the intermolecular potential energy in arbitrary units. EA_{va} and EA_{vv} are the vertical electron affinities of the clusters, i.e. at the intermolecular equilibrium geometry of the neutrals, towards the adiabatic or vertical energy levels of M^-. In step (a) all three electron affinities are negative and no stable MS anions can be observed. In step (b) EA_{va} becomes null and EA_{ad} is positive so that low energy electron can eventually attach in a non Franck–Condon transition towards the ground state of M^- and threshold MS^-_2 anions can be observed which correspond to adiabatic EA values. In step (c) EA_{vv} becomes null so that low energy electron attachment is maximum and MS^-_3 anions are easily formed and detected but their total energy may be too low to allow for evaporation in $MS^-_2 + S$. In that case the threshold number of solvent species corresponds to the vertical electron affinity of M.

atomic partial charges and ε_{ij} and σ_{ij} are the Lennard–Jones coefficients describing the interaction between atoms i and j. We adopt the values of Scheraga et al. [17,18] for ε_{ii} and σ_{ii} and obtain the mixed coefficients from the usual relationships: $\varepsilon_{ij} = \sqrt{\varepsilon_{ii}\varepsilon_{jj}}$ and $\sigma_{ij} = (\sigma_{ii} + \sigma_{jj})/2$. We also use specific coefficients for hydrogen bonds such as X–H . . . Y–A. The attraction between H and Y is increased, as compared to the pure van der Waals interaction, by multiplying the corresponding ε_{ij} by a factor larger than 1 and decreasing σ_{ij}. The repulsion between X and Y or H and A is increased by multiplying the corresponding σ_{ij} by a factor larger than 1 and decreasing ε_{ij}. This method has been proven to give an angular dependence to the hydrogen bond and to give satisfactory results [19,20]. The many-body polarization terms are determined from the following expression:

$$V_i = -\frac{1}{2}(4\pi\varepsilon_0)\alpha_i \vec{E}_i^2$$
$$= -\frac{1}{2}(4\pi\varepsilon_0)\alpha_i \left[\sum_j \frac{eq_j \vec{r}_{ij}}{4\pi\varepsilon_0 r_{ij}^3}\right]^2 \quad (5)$$

where $\vec{E}_i$ is the electric field created by all the atoms of the other molecules on atom i, which mean isotropic polarizability α_i is evaluated from standard bond polarizabilities [21]. The total intermolecular potential energy is then given by:

$$V = \sum_{j>i} V_{ij} + \sum_i V_i \quad (6)$$

which is dependent only on the interatomic distances r_{ij} and the semi-empirical parameters q_i, ε_{ij}, σ_{ij}, and the specific H-bond parameters.

In many empirical models, these parameters are determined by least-square adjustments of the predictions of physical quantities, such as geometry, bond energies or spectral shifts, to the corresponding measured experimental values [17–20]. The obtained partial atomic charges do not necessarily lead to correct values of molecular dipole or quadrupole moments. In this work, many of the solute or solvent molecules we consider are polar and often possess rather large quadrupole moments. In order to get accurate total cluster dipole moments and solvation energies, we thus use partial charges q which reproduce the experimental values of the known isolated molecule dipole moments and/or quadrupole moments when they are available [22]. H bond parameters are then determined in order to reproduce as best as possible the neutral solvation energies of model clusters as given by ab initio calculations or experimental data when available [16]. For anionic species NV we simply distribute the excess electronic charge equally over all atoms which are involved in double bonds. For the molecules studied in this work, the excess electron is indeed expected to be located in a valence π^* orbital of M. With the set of above described potential parameters, we obtain the optimized complex geometries using a genetic algorithm [23]. Examples of such energetically optimized complex geometries are displayed in Figs. 3 and 4, respectively for the neutral and negatively charged adenine–water clusters.

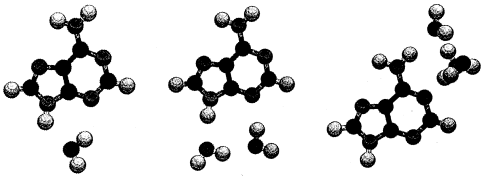

Fig. 3. Optimized structures of adenine–$(water)_{N=1,2,3}$ neutral clusters calculated by means of a semi-empirical model (see text).

2.3. Experiment

We use the Rydberg electron transfer method (RET) which is well-suited for the production of weakly bound valence or dipole-bound anions [15,24–26]. Charge transfer takes place between laser-excited atoms and cold neutral electron-accepting species under well-defined single-collision conditions. The supersonic cluster beam is created by means of a heated pulsed valve (General Valve, 0.15-mm conical nozzle) followed by a heated 1-mm diameter skimmer. We typically expand 1 mbar or less of molecular vapor mixed to few bars of argon, krypton or xenon for the production of mixed molecule-rare gas $M(Rg)_N$ clusters. For the mixed clusters with molecular solvent $M(S)_N$, we use a mixture of few tens of mbars of solvent vapor with few bars of helium as the carrier gas. In order to obtain the molecular vapor, we use a stainless steel oven located just before the pulsed valve which is kept around room temperature for azines and is heated up to 200°C for DNA bases [27]. The molecular cluster beam crosses downstream a beam

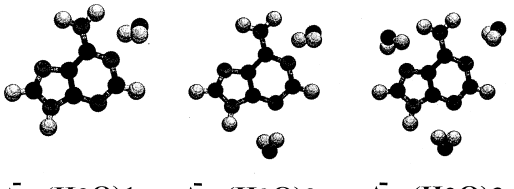

Fig. 4. Optimized structures of adenine–$(water)_{N=1,2,3}$ cluster anions calculated by means of a semi-empirical model (see text).

of xenon atoms, laser-excited in different Rydberg (n, f) levels, and the created anions are further mass-analyzed in a Wiley–McLaren time-of-flight tube and detected by a set of microchannel plates.

Due to the long lifetimes of the Rydberg atoms (typically few μs for $n=25$), the creation time of the observed anions is poorly defined, leading to a rather poor mass resolution. In order to improve it, we introduce a small time delay (1–2 μs) between the laser shot creating the Rydberg atoms and the pulsed extraction voltage of the first acceleration zone. Under those conditions, the resulting mass resolution is of the order of 100. We can also vary the time delay between the pulsed valve opening and the firing of the laser, thus sampling different beam pressures leading to different molecular beam composition in order to optimize the production of the desired anions. The independencies of the rate constants for the formation of created anions are determined by comparison to SF_6^- rate constants due to collisions with a thermal beam [28].

As already shown by several groups [25,26,28], the Rydberg *n*-dependencies of the valence anion formation rates generally exhibit smooth variations over a wide range of *n*-values. At large n values, i.e. for $n>20$–30, formation rates are often constant because the electron transfer process is in most case dominated by a s-wave attachment mechanism with a negligible influence of the Rydberg ionic core [29]. Some exceptions are known for few polar [25] or non-polar molecules [28,30,31] but these should not be however confused with the specific signature of the formation of dipole-bound species [24]. In the present work we have always verified that the observed cluster anions possess a behavior typical for valence negative ions, i.e. that they are constantly formed at large Rydberg quantum numbers *n*.

Table 2
Threshold numbers N_{th} of solvent species S for the observation of stable solvated anions $M^-(S)_N$ where M is a DNA base: the null value for uracil–argon or thymine–argon means that stable valence anions of these two isolated molecules are observed but only when mixed argon clusters are present in the beam (see text)

M\S	M	Ar	Water	Methanol
Uracil/thymine	1	0	1	–
Cytosine	1	–	1–2	2
Adenine	1	–	2	3

3. Results and discussion

3.1. Thresholds for stable valence solvated anions

We have studied the production of stable $M^-(S)_N$ valence cluster anions where M stands for pyridine, pyrimidine, pyrazine, pyridazine (mono and diazines) or for uracil, thymine, adenine, cytosine (DNA bases) and S for Ar, Kr, Xe, water, ammonia, toluene or methanol. Some mixed cluster anions could not be observed, either by lack of neutral cluster parent production or absence of Rydberg electron attachment. The observed threshold numbers N_{th} of solvent species leading to stable valence solvated anions are displayed in Table 1 for azines and in Table 2 for DNA bases. There are some uncertainties in the determination of N_{th}, mainly in the case of rare gas clusters containing more than few units, due to the difficult detection of the actual onset of anion signals, but also in the case of cytosine–water anions which correspond to very weak signals, a consequence of the low vapor pressure of cytosine that we were able to produce without decomposition products.

Qualitatively speaking, for a given molecule M,

Table 1
Threshold numbers N_{th} of solvent species S for the observation of stable solvated anions $M^-(S)_N$ where M is an azine molecule

M\S	M	Ar	Kr	Xe	Water	Ammonia	Toluene
Pyridine	2–3	11±1	–	–	3	4	5
Pyrimidine	1	6±1	5±1	4	1	2	3
Pyridazine	1	2–3	2	1	1	–	–
Pyrazine	1	1	1	1	1	–	–

the threshold number of solvent species N_{th} increases in the order water≤methanol≈ammonia<toluene< xenon<krypton<argon as it can be expected from the polarity and the polarizabilities of these solvent species. Non polar species are indeed less efficient for anion solvation than polar molecules and even less if their polarizabilities are small. For a given solvent species S, larger values of N_{th} correspond to larger solvation energies and thus to a more negative electron affinity of the molecule M (see (3)). This leads to the following ordering for the (negative) electron affinities of azines: pyridine<pyrimidine< pyridazine<pyrazine (see Table 1 for S=Ar). It is slightly different from the experimental ETS data [6,7] from which pyridine<pyridazine< pyrimidine<pyrazine but in agreement with cyclic voltametry experiments [11] and compatible with scaled ab initio calculations [12]. For DNA bases, the ordering is adenine<cytosine<uracil≈thymine (see Table 2 for S=water or methanol) in good agreement with ETS results [10] and Sevilla's calculations [14] but slightly different from Compton's calculations [12] which provide adenine<uracil< cytosine and in total disagreement with cyclic voltametry results [11] where the ordering is cytosine< uracil≈thymine<adenine.

The cases of uracil, thymine and pyrazine are more specifically interesting. We have already reported about uracil [32] for which stable valence anions of the bare molecules have been observed but only when mixed clusters $U(Ar)_N$ are present in the neutral beam, as indicated by the null value of N_{th} in Table 2. When only bare neutral molecules are present in the beam, we only observed dipole-bound negative ions. The same behavior is here observed for thymine molecules so that the same interpretation should hold, i.e. the adiabatic electron affinities of these two molecules are slightly positive while their vertical electron affinities are slightly negative. On the other hand, valence anions of pyrazine are never observed, even when mixed pyrazine–argon clusters are formed. We however observe stable valence anions as soon as only one argon atom is attached to the molecule. This clearly shows that the adiabatic and vertical electron affinities of pyrazine are only very slightly negative. The frontier of the null adiabatic electron affinity should thus be located just in between pyrazine on the negative side and uracil and thymine one the positive side. This is again in contradiction with some of the previous experimental and theoretical data, as displayed in Table 3, and this clearly illustrates the need for more accurate tools.

3.2. Electron affinities

The first hypothesis of the present method is that the cluster anion excess electrons are localized on the molecules M we are interested in and not on the solvent species S. This will be fulfilled if the electron affinity of the solvent subcluster $(S)_N$ is much lower

Table 3
Comparison of the different theoretical (first three columns) or experimental (four last columns) adiabatic EA_{ad} or vertical EA_v electron affinities (in eV) for azines and DNA molecules[a]

M	Younkin [12] EA	Sevilla [14] EA_{ad}	Sevilla [14] EA_v	ETS [6,10] EA	Wiley [11] EA_{ad}	This work S=RG	This work S=mol.
Pyridine	−0.70	−0.39	−0.66	−0.67	−0.21	−0.48	−0.98
Pyrimidine	−0.52	+0.06	−0.26	−0.32	+0.19	−0.37	−0.54
Pyridazine	−	−	−	−0.40	+0.3 1	−0.14	0; −0.49
Pyrazine	−0.30	−	−	−0.07	+0.36	−0.05	0; −0.57
Guanine	−0.94	−0.7	−1.23	−	+1.51	−	−
Adenine	−0.82	−0.3	−0.74	−0.54	+0.95	−	−0.45
Cytosine	−0.03	+0.2	−0.40	−0.32	+0.56	−	0.55
Thymine/uracil	−0.48	+0.3/+0.4 −	0.3/−0.2	−0.29/−0.22	+0.80	≈0	0; −0.30

[a] If not specified, reported EA values are somewhere in between EA_v and EA_{ad}. Our results for EA are separated between those resulting from rare gas atom solvation (S=RG) and molecular solvation (S=mol.) and correspond to mean values (see text) except when only one solvent species has been used, in which case we give only a bracketing.

than that of the molecule M. This condition seems to be reasonable for rare gas solvent atoms which are inert with respect to electron attachment at least for small clusters [33]. Among the molecular solvents that we here use, toluene possesses the largest electron affinity of −1.1 eV [8,9], i.e. still at least 0.5 eV more negative than that of the studied electron attaching species. Closed-shell isolated molecules with only simple bonds such as water, ammonia and methanol are known to possess even more negative electron affinities [3] and to form stable homogeneous cluster anions only for rather large sizes, i.e. $N=11$ for water, N = 35 for ammonia and even much more for methanol [33,34]. We will here consider these molecules as inert solvents with respect to electron attachment as compared to the molecules studied. On the other hand, the excess electron may not be clearly localized in the case of homogeneous clusters $(M)_N^-$, so that the present method would be not relevant.

A second important point to discuss is whether the relevant solvation energies and electron affinities in Eqs. (1–3) are adiabatic or vertical ones. The problem of electron attachment to cold neutral clusters $M(S)_N$ has already been investigated [35] and it has been shown that the solvent plays a multiple role. It can remove energy from the nascent anion M^- and, by breaking symmetry and by adding a large number of intermolecular vibrational levels, it allows attachment of electrons with lower energies and lower partial waves, as compared to the case of the bare molecule. As shown on Fig. 2, one must consider the potential energy diagrams of the $M(S)_N$ and $M^-(S)_N$ systems along two sets of internuclear coordinates: the intramolecular degrees of freedom of the molecule M involved in the electron attachment process and the intermolecular degrees of freedom of the neutral $M(S)_N$ cluster. In our RET experiments we are dealing with very low energy electrons (typically few tens of meV) to cold neutrals (typically 100–150 K for the internuclear coordinates [36]). The attachment process may thus be efficient only close to vertical Franck–Condon transitions in clusters which vertical electron affinities are close to zero, as displayed on Fig. 2. Vertical electron affinities are always more negative than adiabatic ones and vertical anion solvation energies are also less positive than adiabatic ones. Critical cluster sizes for vertical Franck–Condon transitions with null vertical electron affinities are then expected to be larger than those for threshold formation of fully relaxed cluster anions with null adiabatic electron affinities.

On the other hand, even if electron attachment occurs at a larger neutral cluster size, the intramolecular and intermolecular cluster internal energy may lead to evaporation of some solvent species during the interval between the anion creation time and the time at which they are extracted from the collision region for mass analysis, typically 1 μs. This evaporation process cools down the observed cluster anions so that the observed critical cluster sizes N_{th} should indeed correspond to rather cold negative ions and thus adiabatic solvation energies and electron affinities. As a first approximation we thus decide to interpret our experimental threshold cluster sizes with the computed adiabatic solvation energies, keeping in mind that the electron affinities thus derived from Eq. (3) may be more negative than the actual adiabatic electron affinities. Evaporative cooling must be more efficient for rare gas solvents than for molecular solvents, because heats of evaporation from cluster anions are smaller in the atomic case, typically 0. 1 eV, than in the molecular case, with typical values of 0.5–0.7 eV [37,38]. Among results available from our experiments, those obtained with rare gas solvent atoms are thus thought to lead to electron affinities closer to adiabatic values while results obtained with molecular solvent species must be considered only as lower bounds. Table 3 displays the EA values obtained from the threshold cluster sizes of Tables 1 and 2 and the corresponding calculated adiabatic solvation energies displayed in Tables 4 and 5. We use the mean values obtained from Eq. (3) and we separately average over the different atomic solvent species and over the molecular solvent species except for S = M which we discard.

3.3. Discussion

We now discuss each of the above results (in eV) in comparison with previous works (see Table 3). For pyridine, the rare gas value (−0.48) falls in between the ETS value (−0.67) and the value calculated by Sevilla of EA_{ad} (−0.39). On the other

Table 4
Adiabatic neutral (first line) and anion (second line) salvation energies (in eV) corresponding to maximum threshold cluster sizes of Table 1 (second value) and to cluster sizes with one solvent unit less than the minimum threshold value of Table 1 (first value); the third line gives the bracketing for EA values (in eV) as obtained from Eq. (3), i.e. the difference between the first and the second line

M\S	M	Ar	Kr	Xe	Water	Ammonia	Toluene
Pyridine	0.19–0.86	0.45–0.62	–	–	0.58–0.98	0.73–1.04	1.05–1.35
	0.69–1.86	0.87–1.16			1.52–2.18	1.64–2.02	2.03–2.36
	0.50–1.00	0.42–0.54			0.94–1.20	0.91–0.98	0.98–1.01
Pyrimidine	0–0.25	0.19–0.34	0.17–0.36	0.16–0.23	0–0.22	0.16–0.46	0.50–0.78
	0–0.82	0.52–0.75	0.45–0.86	0.42–0.65	0–0.80	0.59–1.11	1.01–1.48
	0–0.57	0.33–0.41	0.28–0.50	0.26–0.42	0–0.58	0.43–0.65	0.51–0.70
Pyridazine	0–0.27	0.05–0.14	0.06–0.12	0–0.06	0–0.24	–	–
	0–0.91	0.14–0.39	0.19–0.37	0–0.20	0–0.73		
	0–0.64	0.09–0.25	0.13–0.25	0–0.14	0–0.49		
Pyrazine	0–0.20	0–0.05	0–0.06	0–0.06	0–0.23	–	
	0–0.73	0–0.14	0–0.18	0–0.19	0–0.80		
	0–0.53	0–0.09	0–0.12	0–0.13	0–0.57		

hand, the molecular value is even smaller (−0.96) than the ETS one and thus seems too low, as expected. For pyrimidine, our two results are closer (−0.37 and −0.54) and intermediate between the Compton's value (−0.52) and the ETS result (−0.32) but much smaller than the Sevilla's adiabatic value (+0.06) and still weaker than a recently reported experimental adiabatic value (−0.24) [39]. Our result for pyridazine (−0.14) is higher than the ETS value (−0.40), but both values for pyrazine agree well (−0.05 and −0.07). Data from cyclic voltametry are always very overestimated. Even if there exists some convergence between others methods, it seems, up to now, that neither theoretical nor experimental methods are able to give reliable accurate electron affinities even for these rather simple molecules.

Table 5
Adiabatic neutral (first line) and anion (second line) solvation energies (in eV) corresponding to maximum threshold cluster sizes of Table 2 (second value) and to cluster sizes with one solvent unit less than the minimum threshold value of Table 1 (first value); the third line gives the bracketing for EA values (in eV) as obtained from Eq. (3), i.e. the difference between the first and the second line

M\S	M	Ar	Water	Methanol
Uracil/thymine	0–0.68	0	0–0.44	–
	0–1.06	0	0–0.74	
	0–0.38	0	0–0.30	
Cytosine	0–0.84	–	0–1.05	0.48–0.97
	0–1.46		0–1.86	0.91–1.64
	0–0.62		0–0.81	0.43–0.67
Adenine	0–0.42	–	0.36–0.77	0.71–1.00
	0–0.73		0.64–1.28	1.09–1.60
	0–0.31		0.28–0.51	0.38–0.60

It is thus not very surprising that DNA bases data are also quite dispersed. Data from reversible reduction potential are again totally off all other results. Our results for adenine (−0.45) and thymine/uracil (≈0) are in between ETS experiments (−0.54 and −0.25) and the Sevilla's values of EA_{ad} (−0.3 and +0.35), but that for cytosine (−0.55) is more negative than all previous results and thus seems to be questionable. We note that, due to the rather high temperature needed to obtain sizable signals (around 200°C), the amino-hydroxy (or enol) tautomer of cytosine may be formed in comparable densities as the usual amino-oxo (or keto) tautomer, even in complexes with water or methanol [40]. The first enol form is however expected to possess a higher electron affinity than the keto form [10] and thus cannot be responsible for our high EA value. Three other experimental studies of DNA bases anions have been recently performed. Bowen's photoelectron spectroscopy experiments [41] have shown that valence anions of the uracil–xenon complex are stable, which is compatible with an adiabatic electron affinity of neat uracil very close to zero. Resonant free electron attachment experiments [42]

also shown that both thymine and cytosine form stable valence anions for low energy electrons. This may suggest that both thymine and cytosine possess positive adiabatic electron affinities. The resonant energy of the attached free electrons is close to zero (0.18 ± 0.15 eV) for thymine, again suggesting a vertical electron affinity close to zero and a slightly positive adiabatic electron affinity. The main resonance is however much higher (1.4 ± 0.15 eV) for cytosine and may be associated with the second attachment energy observed in ETS experiments (1.53 eV [10]). The observed cytosine anions in these experiments may then correspond to long-lived excited negative ion states, which are unlikely to survive in our solvation experiments. Water attachment to DNA bases has been recently studied by Weinkauf et al. [43] by photodetachment photoelectron spectroscopy. Extrapolation of the nucleobase–water cluster affinities down to the isolated monomer base gives small but positive values, also in agreement with our findings about uracil and thymine.

In order to ascertain our data for adenine and cytosine, results from rare gas solvation, as in the case of thymine and uracil, would have been desirable. Despite several attempts, we have not been able to observed such cluster anions presumably because these two DNA bases are more difficult to handle and because more solvent atoms are necessary, as compared to uracil and thymine. It would be interesting to compare the present results obtained with the RET technique and cold neutrals with those obtained by using supersonic ion sources in which cluster anions are produced inside a supersonic expansion and are thus always cold [41].

4. Conclusion

We have studied the stepwise cluster solvation of azine and DNA molecules with negative electron affinities and have been able to observe the threshold number of atomic or molecular solvent species able to definitely stabilize the negative ions. With the help of semi-empirical intermolecular potentials, we have calculated the corresponding neutral and anionic solvation energies, from which we derived an estimate of the electron affinities of the isolated molecules. Even if these results compare fairly well with previous theoretical and gas-phase experimental data, the present method suffers the same ambiguity as the ETS method: it leads to electron affinities which are intermediate between adiabatic and vertical values, depending on the considered solvent and/or molecular species. The story of the determination of gas-phase negative molecular electron affinities seems thus still far from its end.

References

[1] R.N. Compton, Atomic negative ions, in: D. Esaulov (Ed.), Negative Ions, Cambridge Press, 1997, and references therein.
[2] J. Simons, K.D. Jordan, Chem. Rev 87 (1987) 535, and references therein.
[3] R.N. Compton, Negative ion states, in: S.P. McGlynn (Ed.), Photophysics and Photochemistry in the Vacuum Ultraviolet, D. Reidel Publishing, 1985, and references herein.
[4] P.S. Drzaic, J. Marks, J.I. Brauman, in: M.T. Bowers (Ed.), Gas Phase Ion Chemistry, Academic Press, 1984.
[5] S.T. Arnold, J.G. Eaton, D. Patel-Misra, H.W. Sarkas, K.H. Bowen, in: J.P. Majer (Ed.), Ion and Cluster Ion Spectroscopy and Structure, Elsevier, Amsterdam, 1989.
[6] I. Nenner, G.J. Schulz, J. Chem. Phys. 62 (1975) 1747.
[7] D. Mathur, J.B. Hasted, Chem. Phys. 16 (1976) 347.
[8] K.D. Jordan, P.D. Burrow, Acc. Chem. Res. 11 (1978) 341.
[9] P.D. Burrow, A.J. Ashe III, D.J. Bellville, K.D. Jordan, J. Am. Chem. Soc. 104 (1982) 425.
[10] K. Aflatooni, G.A. Gallup, P.D. Burrow, J. Phys. Chem. A 102 (1998) 6205.
[11] J.R. Wiley, J.M. Robinson, S. Ehdaie, E.C.M. Chen, E.S.D. Chen, W.E. Wentworth, Biochem. Biophys. Res. Comm. 180 (1991) 841.
[12] J.M. Younkin, L.J. Smith, R.N. Compton, Theoret. Chim. Acta 41 (1976) 157.
[13] S.W. Staley, J.T. Strnad, J. Phys. Chem. 98 (1994) 116.
[14] M.D. Sevilla, B. Besler, A.O. Colson, J. Phys. Chem. 99 (1995) 1060.
[15] C. Desfrançois, H. Abdoul-Carime, N. Khelifa, J.P. Schermann, J. Chim. Phys. 92 (1995) 409.
[16] C. Desfrançois, in preparation.
[17] F.A. Momany, L.M. Carruthers, R.F. McGuire, H.A. Scheraga, J. Phys. Chem. 78 (1974) 1595.
[18] J. Snir, R.A. Nemenoff, H.A. Scheraga, J. Phys. Chem. 82 (1978) 2497.
[19] K.T. No, O.Y. Kwon, S.Y. Kim, M.S. Thon, H.A. Scheraga, J. Phys. Chem. 99 (1995) 3478.
[20] O.Y. Kwon, S.Y. Kim, K.T. No, Y.K. Kang, M.S. Jhon, H.A. Scheraga, J. Phys. Chem. 100 (1996) 17670.
[21] J.O. Hirschfelder, C.F. Curtiss, R. Byron Bird, Molecular Theory of Gases and Liquids, Wiley, 1954.
[22] D.R. Lide, CRC Handbook of Chemistry and Physics, 74th edn., CRC Press, 1997.

[23] Y. Zeiri, Phys. Rev. E 51 (1995) 2769.
[24] C. Desfrançois, H. Abdoul-Carime, J.P. Schermann, Int. J. Mod. Phys. B 10 (1996) 1339.
[25] F.B. Dunning, J. Phys. B 28 (1995) 1645.
[26] R.N. Compton, Ryberg atom–molecule charge-exchange reactions, in: C. Sandorfy (Ed.), The Role of Rydberg States in Spectroscopy and Reactivity, Kluwer, 1997.
[27] C. Desfrançois, H. Abdoul-Carime, J.P. Schermann, J. Chem. Phys. 104 (1996) 7792.
[28] T. Kraft, M.W. Ruf, H. Hotop, Z. Phys. D 14 (1989) 149.
[29] A. Schramm, J.M. Weber, J. Kreil, D. Klar, M.W. Ruf, H. Hotop, Phys. Rev. Lett. 81 (1998) 778.
[30] T. Kraft, M.W. Ruf, H. Hotop, Z. Phys. D 14 (1989) 179.
[31] C. Desfrançois, N. Khelifa, J.P. Schermann, T. Kraft, M.W. Ruf, H. Hotop, Z. Phys. D 27 (1993) 365.
[32] C. Desfrançois, V. Nriquet, Y. Bouteiller, J.P. Schermann, J. Phys. Chem. 102 (1998) 1274.
[33] P. Stampfli, Phys. Rep. 255 (1995) 1.
[34] J. Jortner, Z. Phys. D 24 (1992) 247.
[35] E. Illenberger, Chem. Rev. 92 (1992) 1589, and references therein.
[36] C. Desfrançois, H. Abdoul-Carime, N. Khelifa, J.P. Schermann, V. Brenner, P. Millie, J. Chem. Phys. 102 (1995) 4952.
[37] C.E. Klots, J. Chem. Phys. 83 (1985) 5854.
[38] C.E. Klots, Z. Phys. D 20 (1991) 105.
[39] P. Chen, R.A. Holroyd, J. Phys. Chem. 100 (1996) 4491.
[40] A. Broo, A. Holmen, J. Phys. Chem. A 101 (1997) 3598.
[41] J.H. Hendricks, S.A. Lyapustina, H.L. de Clercq, K.H. Bowen, J. Chem. Phys. 108 (1998) 8.
[42] M.A. Huels, I. Hahndorf, E. Illenberger, L. Sanche, Chem. Phys. 108 (1998) 1309.
[43] J. Schiedt, R. Weinkauf, D.M. Neumark, E.W. Schlag, Chem. Phys. 239 (1998) 511.